HDL-TR-2107
April 1987

The Theory and Practice of Radiation Dosimetry in the Radiation Hardness Testing of Electronic Devices and Systems

by Klaus G. Kerris

U.S. Army Laboratory Command
Harry Diamond Laboratories
Adelphi, MD 20783-1197

UNCLASSIFIED
SECURITY CLASSIFICATION OF THIS PAGE

AD-A182 980

REPORT DOCUMENTATION PAGE

1a. REPORT SECURITY CLASSIFICATION UNCLASSIFIED	1b. RESTRICTIVE MARKINGS
2a. SECURITY CLASSIFICATION AUTHORITY	3. DISTRIBUTION / AVAILABILITY OF REPORT Approved for public release; distribution unlimited.
2b. DECLASSIFICATION / DOWNGRADING SCHEDULE	
4. PERFORMING ORGANIZATION REPORT NUMBER(S) HDL-TR-2107	5. MONITORING ORGANIZATION REPORT NUMBER(S)
6a. NAME OF PERFORMING ORGANIZATION Harry Diamond Laboratories 6b. OFFICE SYMBOL (If applicable) SLCHD-NW-RI	7a. NAME OF MONITORING ORGANIZATION
6c. ADDRESS (City, State, and ZIP Code) 2800 Powder Mill Road Adelphi, MD 20783-1197	7b. ADDRESS (City, State, and ZIP Code)
8a. NAME OF FUNDING / SPONSORING ORGANIZATION Defense Nuclear Agency 8b. OFFICE SYMBOL (If applicable)	9. PROCUREMENT INSTRUMENT IDENTIFICATION NUMBER
8c. ADDRESS (City, State, and ZIP Code) Washington, D.C. 20305	10. SOURCE OF FUNDING NUMBERS PROGRAM ELEMENT NO. 6.2715H; PROJECT NO.; TASK NO.; WORK UNIT ACCESSION NO.

11. TITLE (Include Security Classification)
The Theory and Practice of Radiation Dosimetry in the Radiation Hardness Testing of Electronic Devices and Systems

12. PERSONAL AUTHOR(S) Klaus G. Kerris

13a. TYPE OF REPORT	13b. TIME COVERED	14. DATE OF REPORT (Year, Month, Day)	15. PAGE COUNT
Summary	FROM Jan 86 TO Jun 86	April 1987	38

16. SUPPLEMENTARY NOTATION
HDL project: 201629, AMS code: P8601-25

17. COSATI CODES		
FIELD	GROUP	SUB-GROUP
09	03	

18. SUBJECT TERMS (Continue on reverse if necessary and identify by block number)
Dosimetry, radiation hardness testing, dose enhancement; thermoluminescent dosimeters; calorimeters; semiconductor detectors; scintillator-photodiode detectors.

19. ABSTRACT (Continue on reverse if necessary and identify by block number)

This monograph covers, in condensed form, the essentials of radiation dosimetry as it is applicable to radiation hardness testing of electronics. An overview of general dosimetry concepts treats absorbed dose and dose rate, charged particle equilibrium, and interface dose enhancement. The most practical techniques for measurement of absorbed dose and dose rate are discussed, both for flash x-ray and cobalt-60 testing. Methods for determining flash x-ray and cobalt-60 spectra are covered briefly. Applications to electronic device testing are discussed with special emphasis on applicable standards. An extensive bibliography is included as an aid for further research. Keywords:

20. DISTRIBUTION / AVAILABILITY OF ABSTRACT	21. ABSTRACT SECURITY CLASSIFICATION
☒ UNCLASSIFIED/UNLIMITED ☐ SAME AS RPT. ☐ DTIC USERS	UNCLASSIFIED

22a. NAME OF RESPONSIBLE INDIVIDUAL	22b. TELEPHONE (Include Area Code)	22c. OFFICE SYMBOL
Klaus G. Kerris	(202) 394-2290	SLCHD-NW-RI

DD FORM 1473, 84 MAR 83 APR edition may be used until exhausted. All other editions are obsolete.

SECURITY CLASSIFICATION OF THIS PAGE
UNCLASSIFIED

CONTENTS

FIGURES

FIGURES (Cont'd)

1. INTRODUCTION

The terms "dosimetry" and "radiation dosimetry" have been used to describe a number of different processes by different authors. Quite generally, dosimetry is the study of how ionizing radiation imparts energy to matter. More specifically, dosimetry is the measurement of absorbed dose in matter at the point of interest. This would be a very satifactory definition, except that it is usually not possible to make this measurement at the point of interest, as I show below. The term "dosimetry" as most commonly used in radiation hardness testing, and the way in which I use it in this report, describes a two-step process:

(a) Measurement of the energy deposited by ionizing radiation per unit mass in a reference material at the point of interest. The reference material may be the actual material present at the point of interest; more commonly it is some other material (i.e., a dosimeter). This measurement serves as a convenient abbreviated description of the radiation at that point (Roesch and Attix, 1968).*

(b) Determination of the absorbed dose in the material at the point of interest (e.g., a particular region in a semiconductor device), using the information found in (a) above.

Steps (a) and (b) are not necessarily always done by the same person or at the same time. Indeed it is quite common for step (a) to be performed by personnel of the radiation facility at which an experiment is performed, whereas step (b) is done by the actual experimenter later on. Nevertheless, the complete process of radiation dosimetry as I define it in this report always requires these two steps.

I begin with a brief overview of the essential radiation dosimetry concepts, followed by sections on measurement of dose rate and spectrum (this is step a), followed by a brief discussion of techniques which can be used to relate these measurements to the actual dose absorbed by a test object of interest (step b).

2. OVERVIEW OF GENERAL DOSIMETRY CONCEPTS

Before going on to a detailed discussion of the process of radiation dosimetry, it will be useful to state a few definitions which are crucial to an understanding of the process.

2.1 Definitions

Absorbed dose (also often called dose or total dose): The mean energy absorbed per unit mass of irradiated material at the point of interest.

*References are listed alphabetically by author at the end of the text.

If $d\bar{\varepsilon}$ is the mean energy imparted by ionizing radiation to matter of mass dm, then (ICRU 1980, ASTM E170)

$$D = d\bar{\varepsilon}/dm \qquad (1)$$

(see fig. 1).

Note that although it is possible to talk about and even rigorously define the absorbed dose in some small region of interest (as the gate insulator of a metal oxide semiconductor device, for example), it is impossible to actually measure the energy imparted to the actual region of interest in the actual test device, $d\bar{\varepsilon}$. This is why all practical dosimetry always requires the two steps (a) and (b) referred to above.

The customary unit of dose is the rad:

$$1 \text{ rad} = 100 \text{ ergs/g} \quad .$$

The SI unit of dose is the gray (Gy):

$$1 \text{ Gy} = 1 \text{ J/kg} \quad ,$$

$$1 \text{ Gy} = 100 \text{ rad} \quad .$$

Although the use of the gray has been strongly advocated by various standards organizations and Government agencies, the rad is used in actual practice by the overwhelming majority of radiation effects experimenters at this time.

Note: Since the absorbed dose depends on the material of interest, the specific material should always be referenced in parentheses right after the name of the unit: e.g., rad(Si), Gy(GaAs), rad(air), etc.

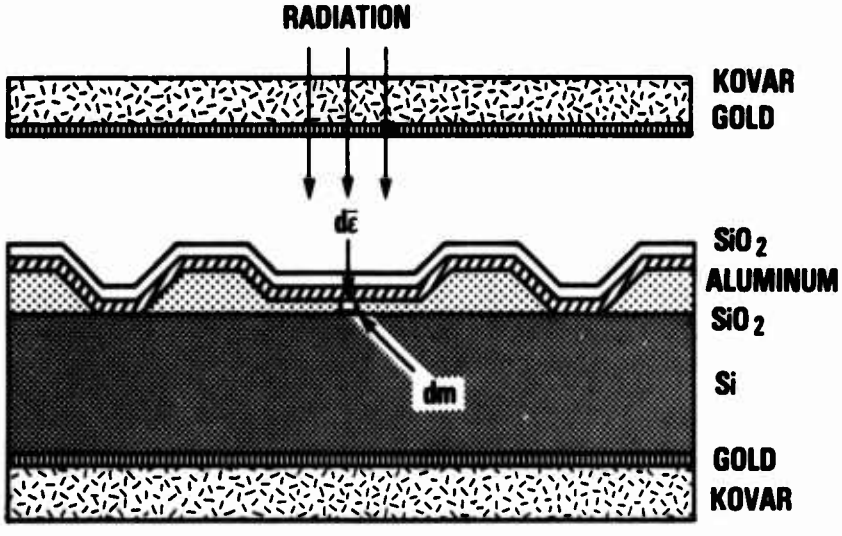

Figure 1. Dose absorbed by region of interest is $d\bar{\varepsilon}/dm$.

Absorbed dose rate (also often called dose rate): The time rate of change of the absorbed dose. If we let dD be the increment of absorbed dose in the time interval dt, then (ICRU 1980)

$$\dot{D} = dD/dt \qquad (2)$$

(see fig. 2).

The units of absorbed dose rate are the rad per second and the gray per second.

Note 1: Since absorbed dose rate is an instantaneous function of time, it is permissible to speak of "the dose rate" when the radiation source is a radioisotope source (Co^{60} for example has a half-life of 5.2 years) because the dose rate is nearly constant for most irradiation time intervals. However, for pulsed radiation sources such as flash x-ray machines, it is necessary to specify where on the pulse the dose rate is measured. In this case when people refer to "the dose rate," they almost invariably mean the dose rate at the peak of the pulse.

Note 2: If the peak height, H_{max}, and the area, A, of a radiation pulse can be determined (say by integration of an oscilloscope trace of the output of a suitable dose rate detector) in consistent units (such as inches and inch-nanoseconds, or whatever), and if we let D be the absorbed dose measured at some point of interest, then it is exactly true that the absorbed dose rate at the peak of the radiation pulse at that point, $\dot{D}_{max}$, is given by

$$\dot{D}_{max} = D(H_{max}/A) \quad . \qquad (3)$$

This is *not* an approximation.

Dosimeter: Any device which can be used to measure absorbed dose (such as a thermoluminescent dosimeter (TLD), dye film dosimeter, calorimeter,

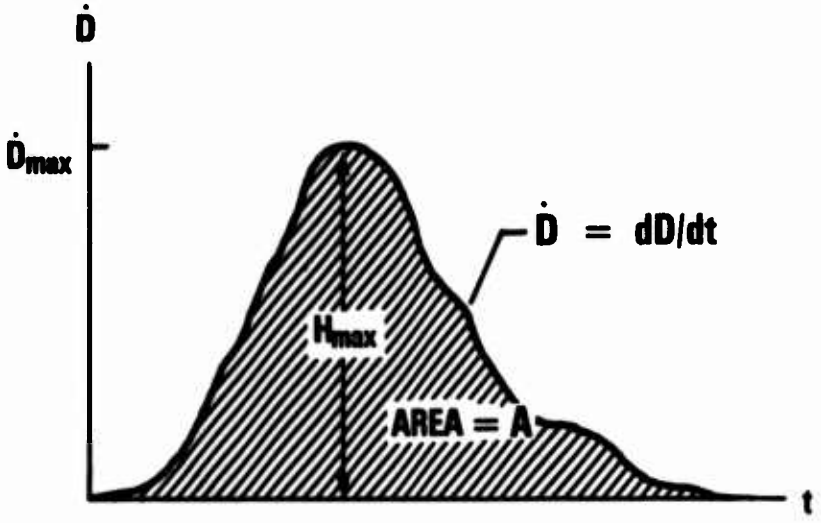

Figure 2. Definition of absorbed dose rate, $\dot{D}$.

or the like). Since this measurement serves to provide a convenient abbreviated characterization of the radiation field at a point (see Introduction), the parameter which is usually measured is the equilibrium absorbed dose in some reference material (usually Si) at that point.

The concept of equilibrium absorbed dose is very important in radiation dosimetry, and is defined in the following paragraphs.

2.2 Charged Particle Equilibrium

Most real-world dosimetry problems are so exceedingly complicated that their exact treatment is either almost impossible or else prohibitively expensive. However, there is one special case which is not only easily manageable theoretically, but which is applicable to a large class of important practical dosimetry problems. This is the case of charged particle equilibrium.

(Note: The analysis which follows is an abbreviated version of the excellent treatment of this topic by Roesch and Attix (1968).)

Let us consider a small volume of material centered at a point P. Let it contain a mass of material Δm. Let this volume of material be traversed by a beam of ionizing radiation. Let ΔE_E be the energy which enters this volume, and ΔE_L the energy which leaves it during some time interval. If there are no nuclear reactions which change the rest mass of Δm, then the energy absorbed by Δm is

$$\Delta E_D = \Delta E_E - \Delta E_L \quad . \tag{4}$$

From the definition of absorbed dose (eq (1)) we see that the absorbed dose in the material of interest can be written

$$D = \Delta E_D / \Delta m \tag{5}$$

or

$$D = (\Delta E_E - \Delta E_L)/\Delta m \tag{6}$$

(see fig. 3a).

Let us now further restrict our analysis to the case of incident photon radiation only. In this case, energy is imparted to matter in a two-step process:

a. Photons impart energy to electrons via the photoelectric, Compton scattering, and pair production processes.

b. Electrons impart energy to matter via excitation, ionization, and elastic scattering processes (see fig. 3b and 4).

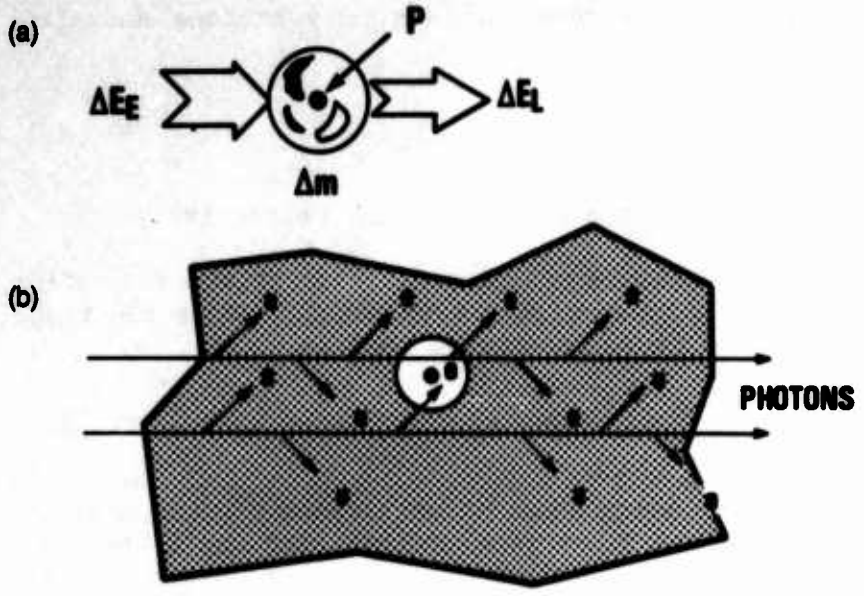

Figure 3. Charged particle equilibrium: (a) energy deposited near a point P; and (b) energy deposited in material by secondary electrons.

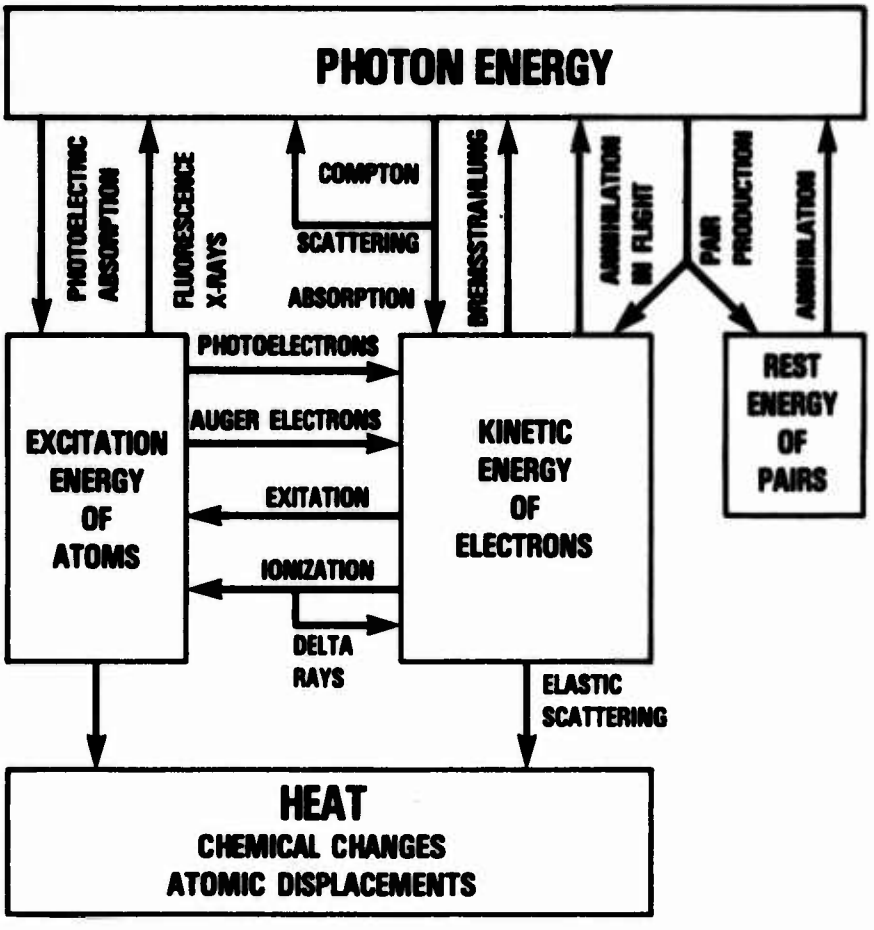

Figure 4. Interactions of energetic photons and electrons with matter (adapted from Hubbell, 1969).

Since the energy deposition process involves only photons and electrons, equation (4) can be rewritten

$$\Delta E_D = \Delta E_E(\gamma) - \Delta E_L(\gamma) + \Delta E_E(e) - \Delta E_L(e) \quad , \tag{7}$$

where the symbols γ and e refer to photons and electrons, respectively.

The condition of charged particle equilibrium (CPE) exists (by definition) when the total energy carried out of the mass element Δm *by electrons* is equal to the energy carried into it *by electrons*, that is,

$$\Delta E_E(e) = \Delta E_L(e) \qquad \text{(for CPE)} \quad . \tag{8}$$

If we consider a thick slab of some homogeneous material (see fig. 5a), we see that an element of volume Δm near the front face of this slab would have more electrons scattered out of it than are scattered into it. CPE does not exist.

As we move the volume element Δm farther into the material slab, we reach a depth (approximately equal to the range of the most energetic secondary electron) where CPE is achieved. This minimum thickness of material required to achieve CPE is commonly called the "equilibrium thickness." (The equilibrium thickness depends on the nature of the material and on the energy spectrum of the radiation.) The condition of CPE applies for this, and greater, material thicknesses (see fig. 5b).

When this condition (CPE) is satisfied, equation (7) simplifies to

$$\Delta E_D = \Delta E_E(\gamma) - \Delta E_L(\gamma) \qquad \text{(for CPE)} \quad . \tag{9}$$

We can now define the equilibrium absorbed dose by combining equations (5) and (9):

$$D_{eq} = [\Delta E_E(\gamma) - \Delta E_L(\gamma)]/\Delta m \qquad \text{(for CPE)} \quad . \tag{10}$$

Equation (10) has an important consequence. $\Delta E_L(\gamma)$ is related to $\Delta E_E(\gamma)$ by the photon absorption equation:

$$\Delta E_L(\gamma) = \Delta E_E(\gamma) \exp[-(\mu_{en}/\rho)\rho\ \Delta x] \quad , \tag{11}$$

where μ_{en}/ρ is the mass energy absorption coefficient of the material of interest, ρ is its density, and Δx is its thickness.

Since the quantity in square brackets is usually quite small, we can use the Taylor series approximation:

$$\exp[-x] = 1 - x + \ldots \tag{12}$$

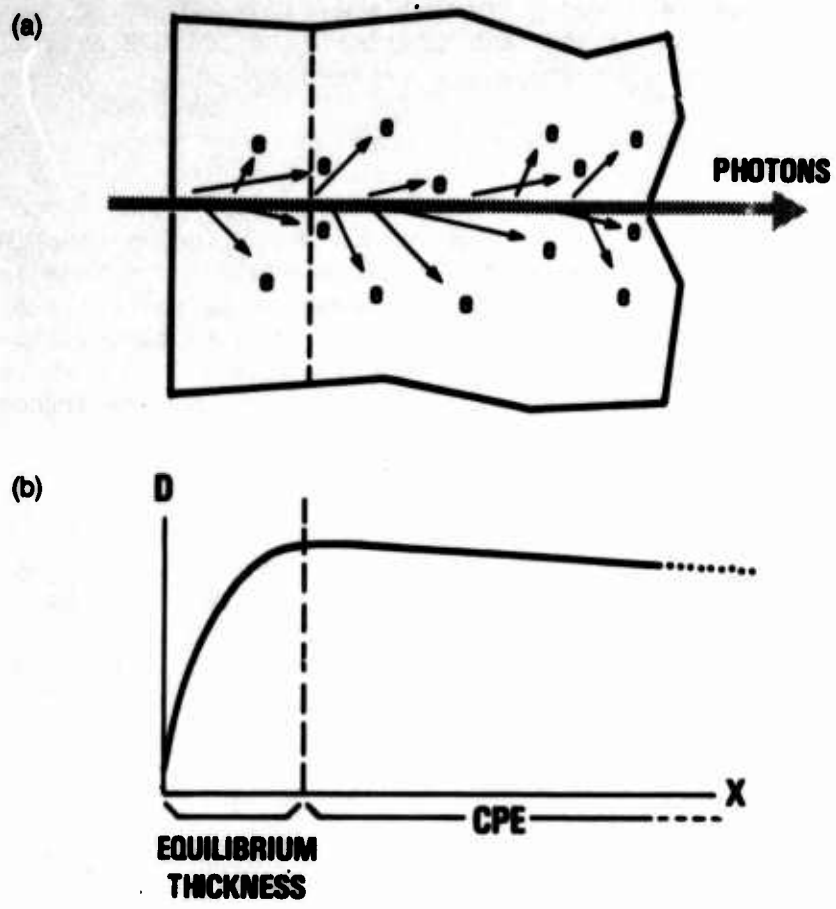

Figure 5. Charged particle equilibrium (CPE): (a) CPE is established at a depth approximately equal to range of secondary electrons; and (b) graph of dose as a function of material thickness.

Equation (11) then becomes

$$\Delta E_L(\gamma) = \Delta E_E(\gamma) - \Delta E_E(\gamma)(\mu_{en}/\rho)\rho\ \Delta x \quad . \tag{13}$$

Using the two relations

$$\rho = \Delta m/\Delta A\ \Delta x \quad ,$$

where ΔA is the area of the volume element, and

$$\Phi_\gamma = \Delta E_E(\gamma)/\Delta A \quad ,$$

where Φ_γ is the photon energy fluence (in MeV/cm^2), equation (13) becomes

$$\Delta E_E(\gamma) - \Delta E_L(\gamma) = \Phi_\gamma(\mu_{en}/\rho)\ \Delta m \quad . \tag{14}$$

Combining equations (10) and (14) gives us the important result that

$$D_{eq} = \Phi_\gamma(\mu_{en}/\rho) \quad \text{(for CPE)} \quad . \tag{15}$$

This implies that if we have two different materials, 1 and 2, exposed to the same photon energy fluence, Φ_γ, and if (and only if) CPE exists, then the equilibrium doses in the two materials are related by

$$D_{eq}(1)/D_{eq}(2) = (\mu_{en}/\rho)_1/(\mu_{en}/\rho)_2 \quad \text{(for CPE)} \quad . \tag{16}$$

Equation (16) shows why the concept of equilibrium dose is so important to practical dosimetry. For if we can measure the equilibrium dose in some reference material, 2, then we can calculate what the equilibrium dose in some other material of interest, 1, would be in the same radiation field by using equation (16). If the measurement in material 2 is of some nonequilibrium dose, then we cannot say anything about the dose in material 1. It is therefore crucial to be able to measure the equilibrium dose in a reference material.

2.3 Measurement of Equilibrium Dose

If we wish to measure the equilibrium dose in some material, say silicon, figure 5b makes it pretty clear (at least in principle) how to do that. We simply surround a small silicon absorbed energy detector with an equilibrium thickness of silicon. This is shown schematically in figure 6a. The energy absorbed by the small Si detector divided by its mass is the silicon equilibrium dose at the center of this "dosimeter."

Now, although the arrangement of figure 6a can actually be used as shown (if a thermistor were added to the small Si "detector" to measure its temperature rise, fig. 6a would show a "total dose" silicon calorimeter), such an arrangement is often cumbersome and difficult to implement in practice.

What is more commonly done (because it is much easier) is to surround a passive dosimeter (such as a thermoluminescent dosimeter, or TLD) with an equilibrium shield of some material. Typically neither the TLD nor the surrounding equilibrium shield are made of the material of interest (silicon in our example). Figure 6b shows a common arrangement where the TLD is manganese-doped calcium fluoride (CaF_2:Mn) and the equilibrium shield is aluminum. If such a dosimeter is used to measure silicon equilibrium dose, attention must be paid to the energy spectrum of the photon source, and care must be exercised in the choice of materials used for the following reason. The arrangement shown in figure 6b technically consists of a Bragg-Gray cavity (Burlin, 1969, 1970), in this case a small cavity filled with CaF_2:Mn surrounded by Al. According to cavity theory, the dose in the wall material (Al) can be readily related to the measured dose in the cavity material (CaF_2:Mn) only in these two limiting cases:

(a) If the cavity is much thinner than the range of the secondary electrons produced in the wall material, then

$$D_{wall} = [S_{wall}/S_{det}]D_{det} \quad , \tag{17}$$

where S is the electron mass stopping power ($S = (dE/dx)/\rho$).

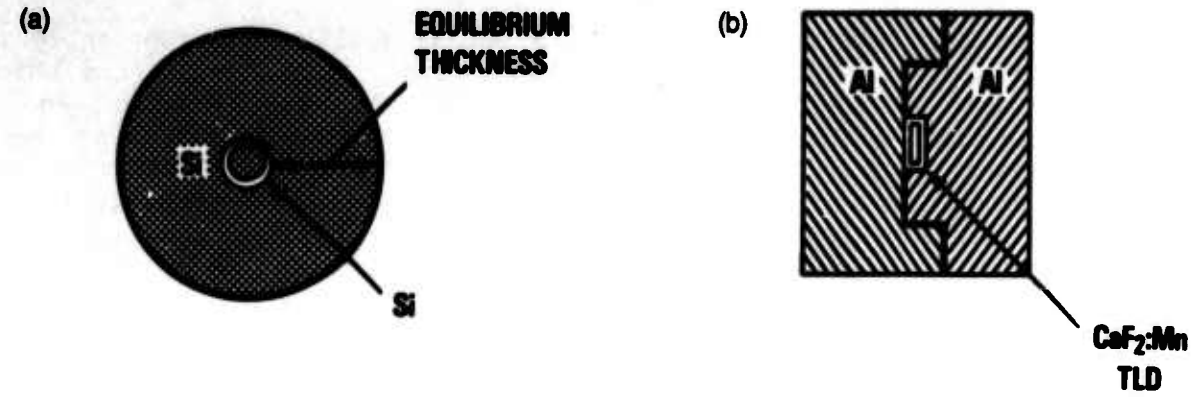

Figure 6. Measuring equilibrium dose: (a) idealized dosimeter and (b) practical implementation.

(b) If the cavity is much thicker than the range of the most energetic secondary electron produced in the wall material, then CPE is reestablished in the cavity material, and equation (16) applies:

$$D_{wall} = [(\mu_{en}/\rho)_{wall}/(\mu_{en}/\rho)_{det}]D_{det} \quad . \tag{18}$$

Unfortunately, the cavity dimension is usually somewhere between these two limiting cases, and there is no simple way to relate D_{wall} to D_{det}. Further, since what is really desired is the equilibrium dose in some other material of interest, say Si, equation (16) must be used one more time:

$$D_{Si} = [(\mu_{en}/\rho)_{Si}/(\mu_{en}/\rho)_{wall}]D_{wall} \quad . \tag{19}$$

It should be clear by now that a dosimeter of the type illustrated in figure 6b can only be used to measure the equilibrium dose in some reference material if the two following conditions are both satisfied:

(1) The photon source spectrum must be known well enough so that all stopping power ratios and abscrption coefficient ratios in equations (17) to (19) can be calculated, *and*

(2) one of the following three conditions is true:

(a) one of the two limiting cases applies so that equation (17) or (18) can be used, or

(b) the photon energy spectrum is such that all the stopping power ratios and absorption coefficient ratios are unity in the energy region covered by the spectrum of the incident photon radiation, or

(c) the dose is calculated using a full-scale coupled electron-photon transport calculation.

As mentioned before, option 2a is seldom applicable. Option 2c is very undesirable, but is sometimes necessary, especially for sources which have significant photon energy components below 200 keV. Option 2b is fortunately applicable for a significant number of cases, namely those where the photon energy is mostly above 200 keV. (See fig. 7 and 8 for plots of absorption coefficient ratios and stopping powers versus photon energy.) The practical applications of this to radiation hardness testing are covered in sections 3 and 4.

2.4 Interface Dose Enhancement

One last dose-related phenomenon must be discussed here which is of crucial importance to the process of deducing the absorbed dose in a region of interest in a device from an equilibrium dose measurement made by a dosimeter. This is the phenomenon of interface absorbed dose enhancement (also frequently called interface dose enhancement, or simply dose enhancement).

Consider a layered structure of two dissimilar materials, say silicon and gold, each several equilibrium thicknesses thick, exposed to a beam of photon radiation. Applying the equilibrium dose relationship (eq (16)) to this situation, we would expect the dose in the gold layer to be higher than the dose in the silicon layer by the ratio of the respective mass energy absorption coefficients, and we would expect there to be a discontinuity in

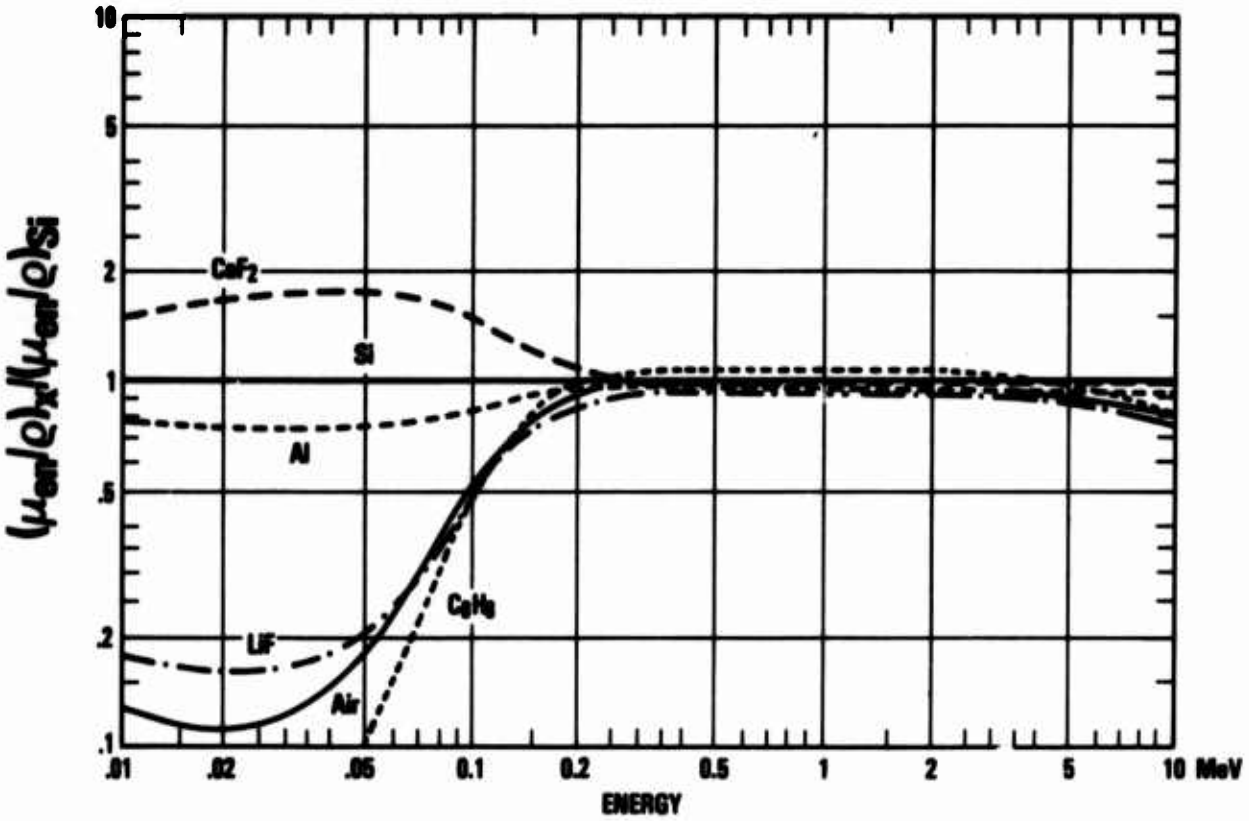

Figure 7. Ratio of $(\mu_{en}/\rho)_x/(\mu_{en}/\rho)_{Si}$ versus photon energy.

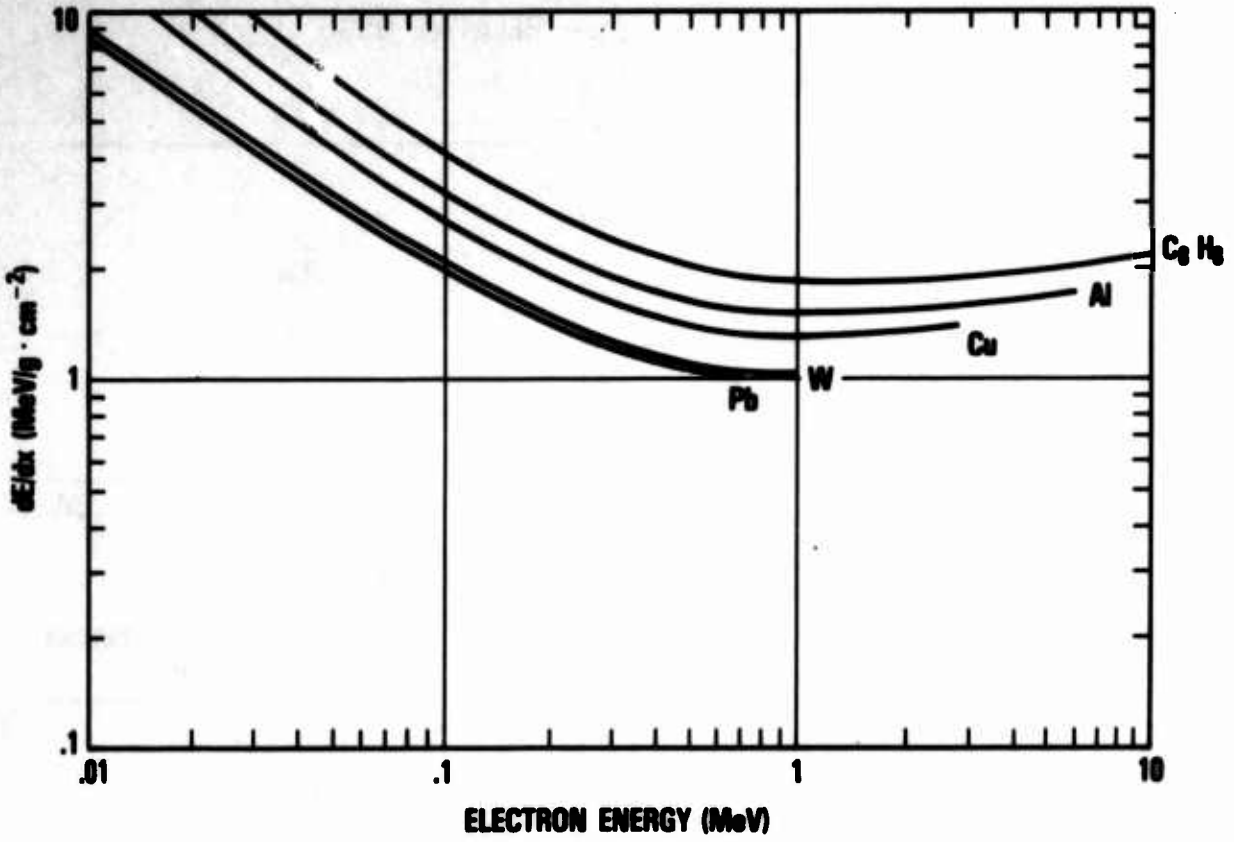

Figure 8. Electron mass stopping power versus electron energy for various materials.

the dose at the interface. This hypothetical situation is shown in figure 9a for the case of 1-MeV photons. However, equation (16) does not consider nonequilibrium electron transport across the interface. When this is properly taken into account, we get the situation shown in figures 9b-c, which are the result of an energy deposition calculation near an Si/Au interface for incident 1-MeV photons, using the Monte Carlo transport code TIGER (Halbleib and Melhorn, 1984). (There are many published references to this phenomenon; for examples, see Burke and Garth, 1976; Chadsey, 1978; Garth et al, 1975; Long et al, 1982; and Wall and Burke, 1970.)

The ratio of the actual dose at a point in a material to the equilibrium dose in that material is called the dose enhancement factor, F_{DE}. In figure 9b, for example, the dose enhancement factor in Si at the Si/Au interface is 1.64; in figure 9c the dose enhancement factor in Au at the Au/Si interface is 0.66. Figure 10, which is reproduced from Garth et al (1975), shows F_{DE} in Si near an Si/Au interface. Note that F_{DE} depends very strongly on photon energy, on the distance from the interface, and, for energies >400 keV, also on the direction of the photons.

It must be noted that figures 9 and 10 give upper limits to the dose enhancement factor which might be expected in a real device because they show the relative dose at an interface between two thick layers. In a typical

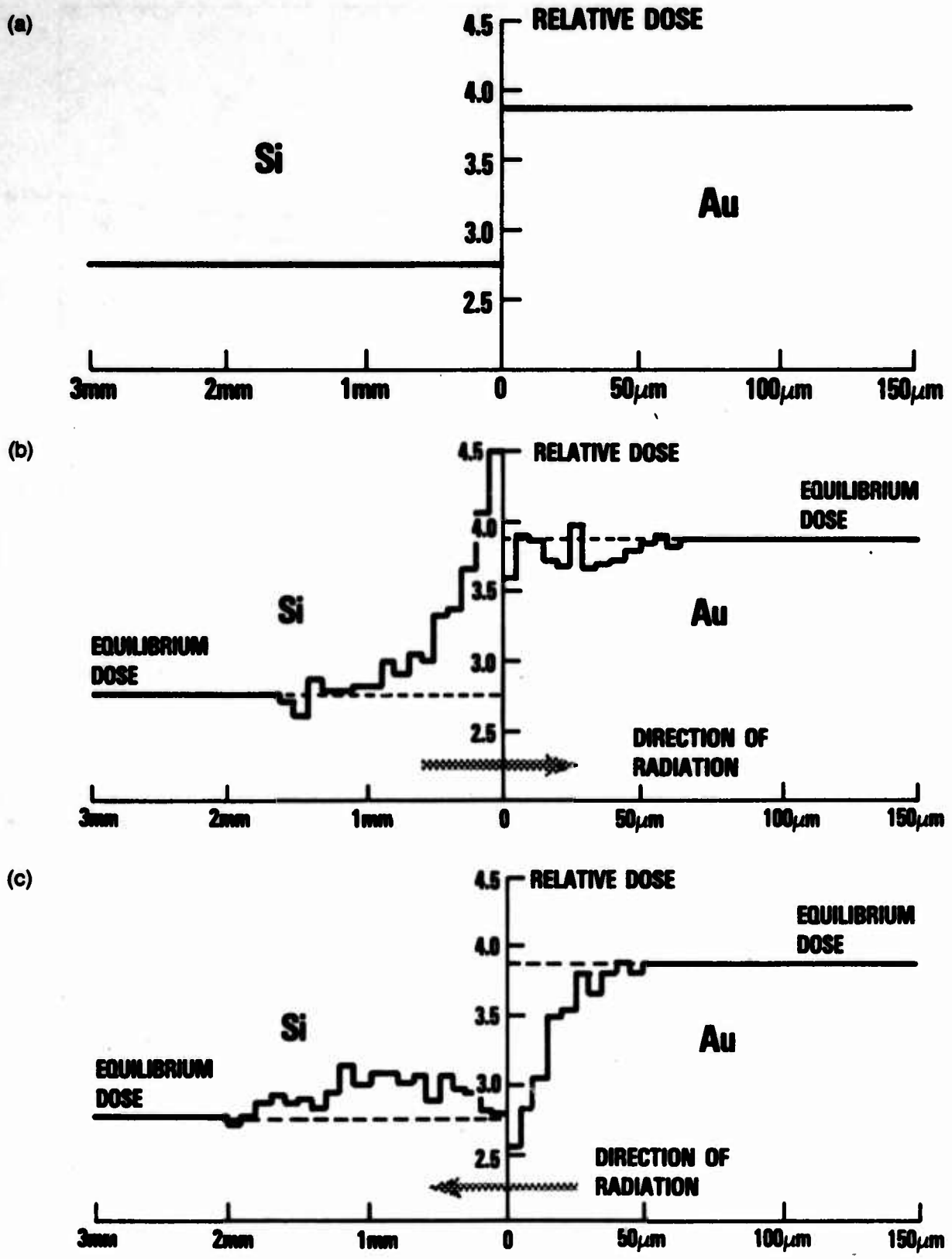

Figure 9. Relative dose at interfaces (a) without and (b, c) with dose enhancement.

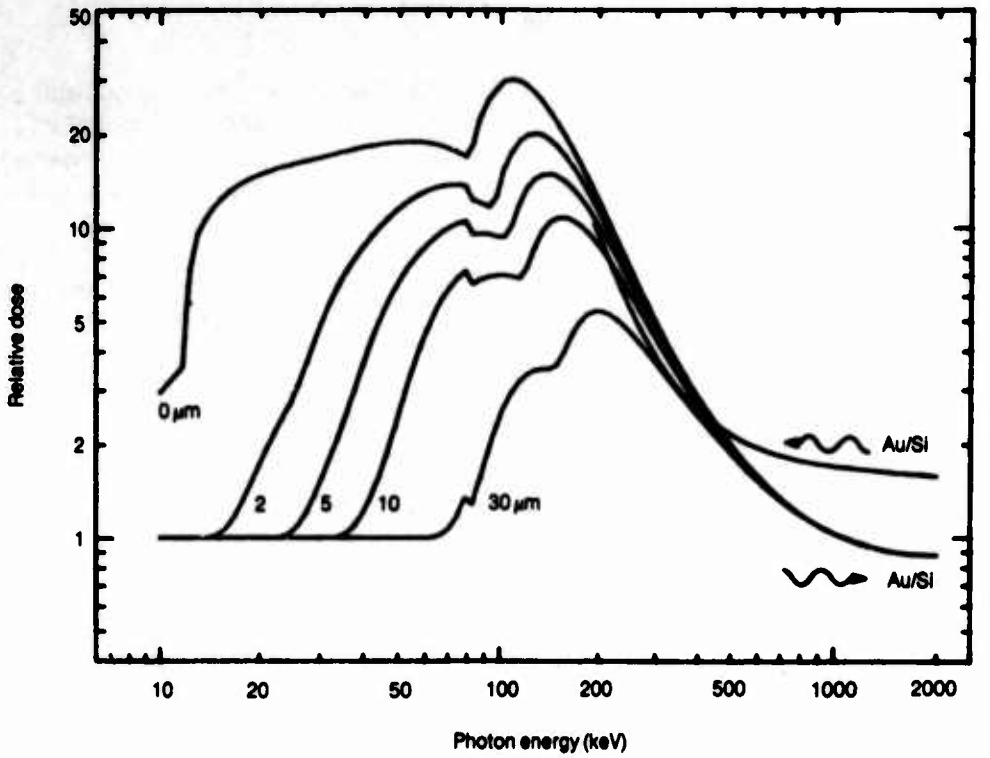

Figure 10. Relative dose versus photon energy for Au/Si interface (from Garth et al, 1975).

semiconductor device (such as the one shown schematically in fig. 1) most of the interfaces are between layers of dissimilar materials which are much less than an equilibrium thickness. In that case the situation becomes much more complex because all electron transport is nonequilibrium, and the energy deposited at or near an interface can come from electrons which originated in materials which may be several layers removed from the interface in question. Calculating the dose in such a device from the equilibrium dose as measured by a dosimeter is very difficult; however, section 6 gives some procedures which may be employed to minimize dose enhancement effects and the attendant dosimetry uncertainties.

Specific techniques for measuring silicon equilibrium dose and dose rate are covered in the following two sections. Once the silicon equilibrium dose is known it is still necessary to relate this dosimeter dose to the dose in a particular region of the device under test. Techniques for doing this are discussed in section 6.

3. MEASUREMENT OF ABSORBED DOSE

The most commonly used dosimeters for absorbed dose (total dose) measurements in radiation hardness testing at cobalt-60, flash x-ray, and linac facilities are the thermoluminescent dosimeter (TLD), the calorimeter, and the radiachromic dye film dosimeter. Each of these systems is discussed below.

3.1 Thermoluminescent Dosimeters

TLD's are very popular dosimeters because they are small, passive (requiring no instrumentation during irradiation), and inexpensive, and they retain accurate dose information for long periods of time (years) between irradiation and readout. The useful dose range of TLD materials is $\sim 10^{-2}$ to $<10^{6}$ rad (10^{-4} to $<10^{4}$ Gy).

A large variety of materials is available for thermoluminescence dosimetry; however, the overwhelming favorites are lithium fluoride (LiF), manganese-activated calcium fluoride (CaF_2:Mn), and dysprosium-activated calcium fluoride (CaF_2:Dy). The dosimeters are available as powder, blocks made from extruded polycrystalline material, and discs consisting of very fine powder uniformly dispersed throughout a polytetrafluoroethylene (PTFE, Teflon) matrix. A common size of extruded block is 0.125 × 0.125 × 0.035 in., produced by the Harshaw Chemical Co.* A commonly used size of Teflon dosimeter is a disc, 6 mm in diameter and 0.4 mm thick, made by Teledyne-Isotopes Inc.†

The thermoluminescence process.--All thermoluminescent materials consist of a crystalline insulator material with added dopants which introduce stable electron traps in the forbidden band gap. Ionizing radiation creates electrons and holes in the valence band which are trapped in the band gap. The density of filled traps is proportional to the dose absorbed by the material. Subsequent heating of the material empties some of the electron traps, allowing electrons from F-centers to recombine with free holes at luminescence centers, emitting light. The integrated light output is proportional to the density of filled traps, and therefore to the absorbed dose in the TLD material. This process is illustrated in simplified form in figure 11 for LiF activated with magnesium and titanium.

Instrumentation.--Readout of TLDs is accomplished by a special-purpose instrument consisting of a programmed heater, optical system, and photomultiplier detector to measure the light emitted by the TLD during a predetermined heating cycle, and an integrating picoammeter which can measure the current or the charge from the photomultiplier. The total integrated charge from the photomultiplier during part or all of the heating cycle is usually related to the absorbed dose in the dosimeter. TLD readout instruments are commercially available from the Harshaw Chemical Co., Teledyne-Isotopes, Inc., and others.

Choice of material.--The choice of the specific TLD material and capsule material and thickness to be used depends on the specific application. For high-energy photon sources ($h\nu \geq 200$ keV) such as high-voltage flash x-ray generators and Co^{60} and Cs^{137} sources, and where the quantity of interest is Si equilibrium dose (as in most radiation hardness testing), a good combination of materials is a CaF_2:Mn TLD in an Al equilibrium shield. The reasons for this can be found by reference to figures 7 and 8. For the materials and

*Harshaw Chemical Co., Crystal & Electronic Products Dept., 6809 Cochran Rd., Solon, Ohio 44139.
†Teledyne-Isotopes, 50 Van Buren Ave., Westwood, New Jersey, 07675.

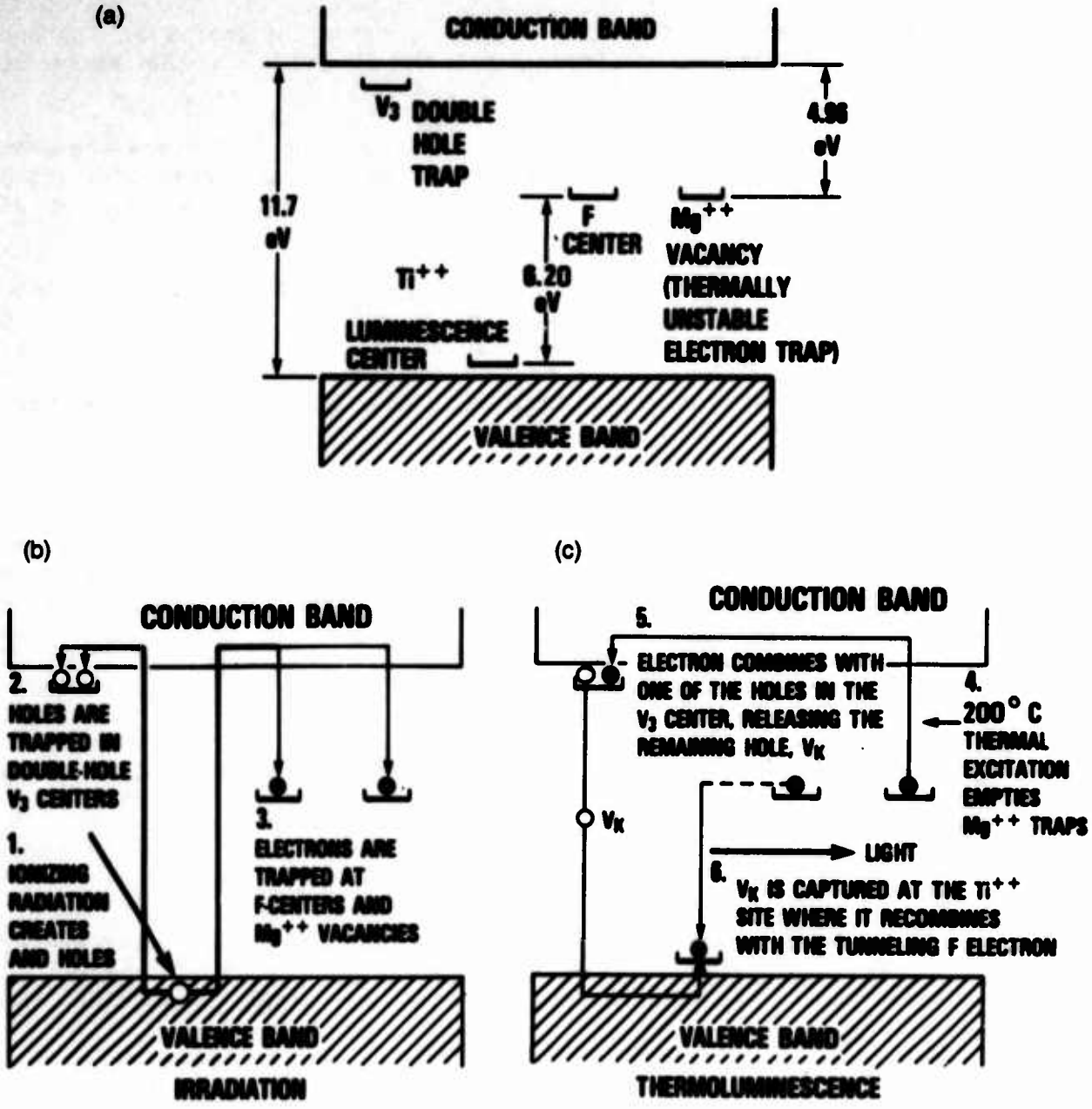

Figure 11. Thermoluminescence process: (a) simplified band model of LiF:Mg,Ti, (b) irradiation, and (c) thermoluminescence. (Adapted from Becker, 1973, p 45.)

photon energies mentioned above, all relevant mass absorption coefficients and mass stopping powers are so close to those of silicon that the silicon equilibrium dose can be determined using simple Bragg-Gray cavity theory. Also, the response of CaF_2:Mn is nearly linear with dose and, once exposed, the dosimeters retain their information for a long time with a small and well-known fading correction (Gorbics et al, 1973).

For radiation sources which have a significant part of their energy spectrum below 200 keV, more detailed calculations are necessary regardless of

which material is chosen for the TLD. In these cases the choice of TLD and capsule material is largely arbitrary, and can be made on the basis of convenience, cost, etc.

The choice of whether powder, extruded blocks, or PTFE discs are used is also primarily one of convenience and cost. Some of the trade-offs which should be considered in making this decision are examined by Gorbics et al (1973).

General references to the theory and practice of thermoluminescence dosimetry can be found in Attix (1970), Becker (1973), Cameron (1970), and Fowler and Attix (1966). For guidance and specific instructions on the proper procedures in the use of TLD systems for determining absorbed dose in radiation hardness testing of electronic devices, there are no better references than ASTM Standards E665, E666, and E668.

3.2 Calorimeters

In principle, calorimetry is the most direct method for measuring the dose in a reference material. The calorimeter makes use of the fact that when a mass of material, Δm, absorbs a quantity of heat, ΔE, the resulting temperature rise is given by

$$\Delta T = (1/C_p)(\Delta E/\Delta m) \qquad (20)$$

where C_p is the specific heat at constant pressure. Since $\Delta E/\Delta m = D$ by equation (5), we see that

$$D = C_p \Delta T \quad . \qquad (21)$$

If we know the specific heat of a material, and provided that all the energy deposited by ionizing radiation goes into heat and not chemical changes or atomic displacements, we can determine dose by simply measuring the temperature rise.

Other advantages of calorimeters are that they offer a wide choice of reference materials in which to measure dose (as opposed to the very limited selection of available thermoluminescent phosphors), their response is independent of the absorbed dose rate, and the conversion of absorbed energy to heat takes place almost instantaneously (in ~10 ps or so).

There are also a number of disadvantages associated with calorimeters:

(a) Calorimeters are not commercially available (as TLD's and dye films are). They must be carefully designed for each specific application to have the proper dose range, and to avoid thermal losses and other thermal defects.

(b) Calorimeters are not passive detectors. Each calorimeter requires an active instrumentation channel capable of measuring signals in the microvolt range, which is protected from electromagnetic interference.

(c) The practical dose range of calorimeters is rather more restricted than that of TLD's. The lower level of detectability is constrained by temperature measurement techniques. For Si, $1/C_p \approx 1.4 \times 10^{-5}$ °C/rad at 25°C. The thermoelectric voltage for an iron-constantan thermocouple is 52 μV/°C at 25°C, leading to a sensitivity of 7.3×10^{-4} μV/rad. If 10 μV could be measured reliably, then the lower limit of detectability of such a calorimeter would be ~10^4 rad. If a thermistor with a temperature coefficient of resistance of ~10^3 Ω/°C (R ≈ 25 kΩ at 25°C) were used instead of a thermocouple, the sensitivity of the calorimeter would be ~1.4×10^{-2} Ω/rad. If a ΔR of a few ohms out of 25 kΩ is measurable, then doses as low as ~100 rad would be measurable with this calorimeter. The upper limit of detectability is quite high, since it is principally constrained by the ability of the absorber or the temperature sensor to survive thermomechanical damage.

The principal application for calorimeters is dosimetry at large flash x-ray facilities with fairly low-energy photon spectra, typically those with accelerating voltages of 1.5 MV or less.

Two types of calorimeter are often distinguished in the flash x-ray community: the "dose" calorimeter and the "fluence" calorimeter. The "dose" calorimeter (at least in principle) consists of an absorber which is thin enough so that the energy deposition is uniform throughout its depth. At high enough energies there will also be sufficient material surrounding the absorber to establish charged particle equilibrium. This is essentially the situation depicted in figure 6a. This arrangement measures equilibrium dose. The "fluence" calorimeter derives its name from the fact that it measures not dose, but the incident photon energy fluence, Φ_γ (in MeV/cm^2). This is accomplished by making an absorber thick enough to absorb all (i.e., ~95 percent) of the incident photon energy and carefully defining the active area of the absorber. Corrections for the remaining unabsorbed energy can be made analytically, but the spectrum must be known. The "fluence" calorimeter is frequently used for very low energy spectra, that is, on accelerators with an accelerating voltage of ~250 kV or less.

The two types of calorimeter are shown schematically in figure 12 (which shows, in simplified form, two types of calorimeter in use at Maxwell Laboratories, Inc., courtesy of J. Rauch).

3.3 Photochromic Dosimeters

Photochromic dosimeters are based on organic dyes which change their color or optical density or both when exposed to ionizing radiation. Two very common types of photochromic dosimeters are (1) radiachromic dye film dosimeters which consist of aminotriphenylmethane dye derivatives, stabilized and sensitized in solid solution in nylon, commonly produced as 0.001-in.-thick film, and (2) red Perspex 4034, a dyed polymethyl methacrylate sheet.

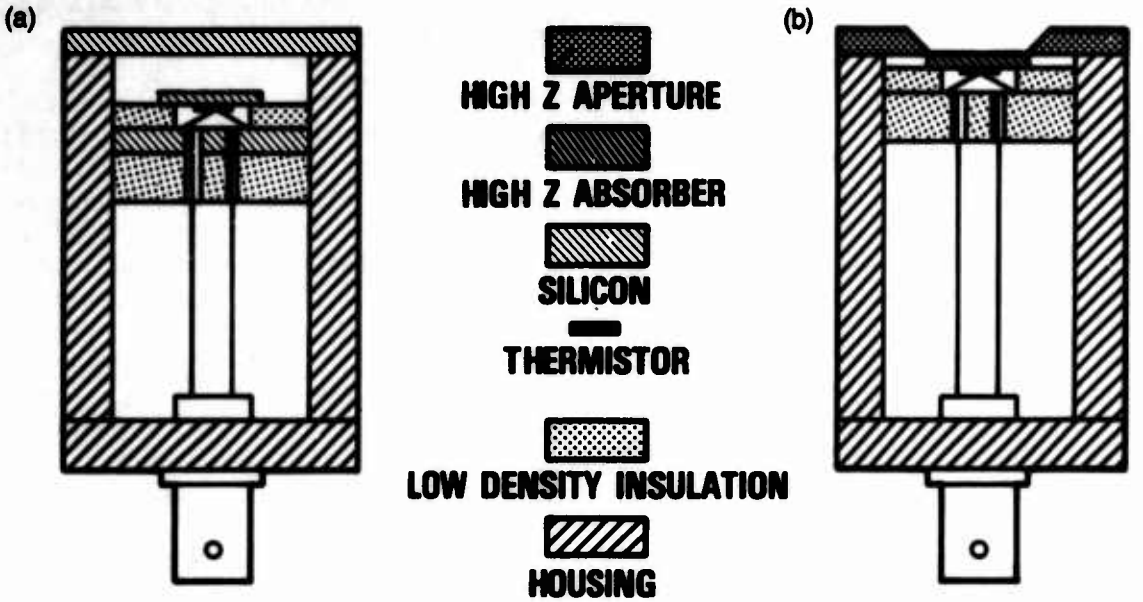

Figure 12. Typical calorimeters (schematic): (a) "dose" calorimeter and (b) "fluence" calorimeter.

Radiachromic dye dosimeters have a useful dose range of about 10^4 to 10^7 rad. This dose range, coupled with the fact that the dosimeter is passive and the color change is stable over extended periods of time, makes radiachromic dye film dosimeters particularly useful for very high absorbed dose irradiations in radioisotope irradiators such as Co^{60} or Cs^{137}.

In use, the optical density of the unirradiated dye film dosimeter is measured with a spectrophotometer. The dosimeter is exposed in a suitable equilibrium shield. The optical density is again determined. The absorbed dose is proportional to the change in the optical density.

Dye film dosimeters are very useful in applications where detailed absorbed dose distributions must be determined over relatively large (tens or hundreds of square centimeters) areas. For this application the dosimeter is not used in the form of small discrete chips, but rather as a continuous sheet which can be evaluated in two dimensions with a scanning microspectrophotometer.

Dye film dosimeters are not as widely used in radiation hardness testing as TLD's or calorimeters. Their principal application is in the fields of radiation processing, sterilization, and food irradiation.

(More information on radiachromic dye dosimeters can be found in work by McLaughlin and Chalkley (1965) and McLaughlin (1970, 1982). The only commercial source of radiachromic dye dosimeters at the present time is Far West Technology, Inc., 330-D South Kellogg, Goleta, CA 93017. More information on red Perspex dosimetry is given by Whittaker (1970).)

4. MEASUREMENT OF ABSORBED DOSE RATE

In order to be useful as an absorbed-dose-rate measuring device, a detector must faithfully reproduce the time rate of change of the absorbed dose in the reference material of interest throughout the history of the radiation pulse. To do that it must have all the following attributes:

(a) Energy response: The detector material must either have the same energy response function as the reference material, or its energy response must be relatable to that of the reference material over the spectral energy range in question by equation (16).

(b) Time response: All the time constants of the detector must be shorter than the fastest frequency component of the radiation pulse.

(c) Linearity: The response of the detector (current or voltage versus dose rate) must be linear up to the highest expected dose rate in the radiation pulse.

Any detector which satisfies these criteria can be used in one of two modes:

(1) It can be calibrated so that its electrical output is in some known proportion to the absorbed dose rate in the reference material. The detector can then be used to measure the dose rate as a function of time directly at a point of interest.

(2) If it is desired to know the dose rate at a number of locations, but it is undesirable to implement that number of active instrumentation channels, the detector can be used as a pulse shape monitor at a typical location: that is, a location where the pulse shape is known to be or may reasonably be expected to be the same as at the locations of interest. If the absorbed dose is measured at all the locations of interest with a passive dosimeter (a TLD, say), then the dose rate at all these locations may be determined by using equation (3) with D as measured by the TLD's and the pulse shape characteristics as given by the single dose-rate detector.

The most widely used devices for absorbed dose rate measurements in radiation hardness testing of electronics are semiconductor detectors such as PIN diodes, scintillator-photodetector combinations, and secondary emission detectors. Each of these devices is discussed below.

4.1 Semiconductor Detectors

Typically a semiconductor detector consists of a reverse-biased silicon diode with a circuit to measure the photocurrent. The diode may be a silicon PIN junction as shown in figure 13; it may be a simple silicon junction diode.

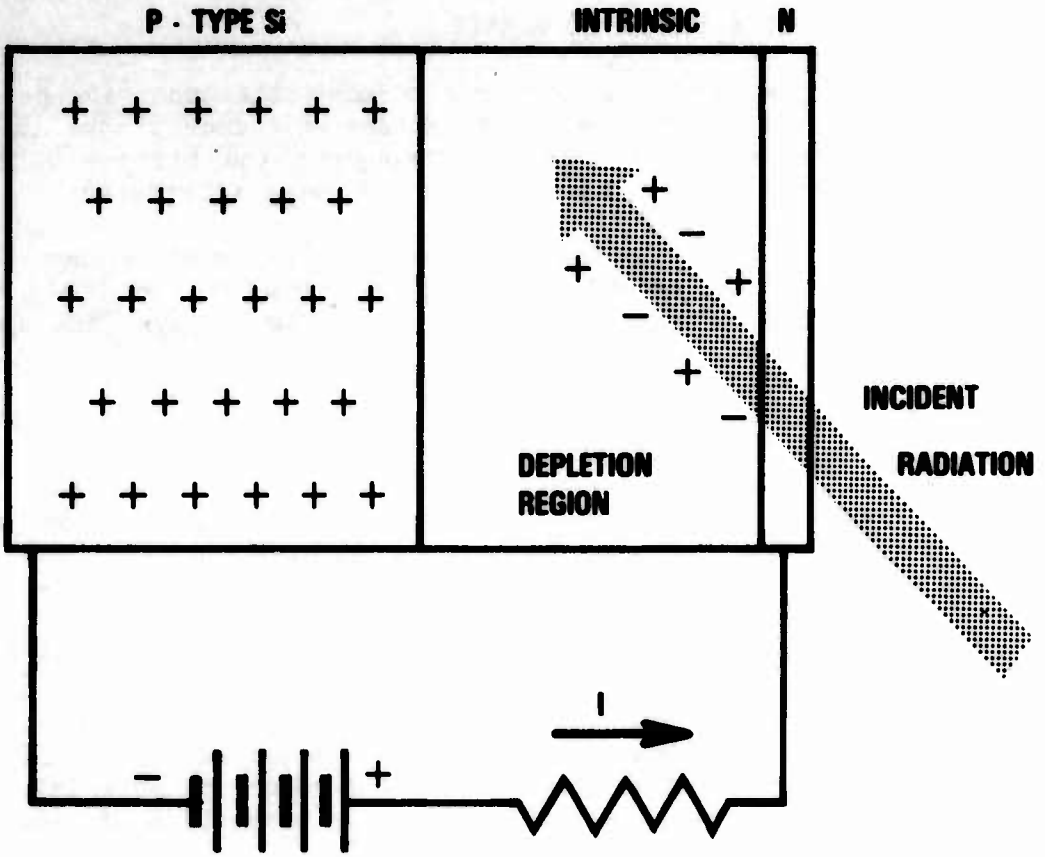

Figure 13. Silicon PIN junction detector.

Characteristics of semiconductor detectors are as follows:

(a) Energy response: If the reference material of interest is silicon, then of course the energy response of an Si detector is perfectly matched to that of the reference material. CPE must still be established; this is particularly important for high-energy photon spectra.

(b) Time response: A typical large PIN diode (1-cm² area, 250-μm depletion layer thickness, 850-V bias) has a step function response of 7.0 ns, and a frequency response of 47.7 MHz. Smaller diodes would have shorter rise times and higher frequency response, but a smaller dynamic range.

(c) Linearity: The response of a reverse-biased semiconductor detector will be linear as long as the voltage developed across the load resistor by the photocurrent is less than the bias voltage (say $I_{pp}R_L \leq V_{bias}/2$). The linear range of a semiconductor detector must be determined from its measured sensitivity ($A/rad \cdot s^{-1}$) or from manufacturer's data sheets. Linear operation up to 10^9 rad(Si)/s is readily obtainable.

The relevant operating parameters (calibration constant, dynamic range, linearity, and time response) of PIN junction detectors specifically designed for dose-rate measurements are usually supplied by the manufacturer.

If an ordinary silicon junction diode is used, these parameters are usually not available. In this case it is necessary for the experimenter to characterize the operation of the diode over the entire parameter space (energy, pulse shape, and dose rate) in which it will be used in order to obtain satisfactory results.

4.2 Scintillator-Photodiode Detectors

The principle of operation of this type of detector is shown diagrammatically in figure 14. Ionizing radiation is absorbed by a scintillator which emits a pulse of light of an intensity proportional to the absorbed dose rate. The light is converted to an electrical current pulse by a photodetector which is optically coupled to the scintillator.

A typical plastic scintillator (pilot-B) consists of a solid transparent solvent (polyvinyl toluene) containing a scintillator (p-terphenyl which emits light at 340 nm) plus a wavelength shifter (p,p'-diphenyl stilbene) which absorbs the light from the scintillator and reemits it at a wavelength (408 nm) which is better matched to the photodetector response.

A common photodetector is the planar vacuum photodiode (such as ITT FW-114 or FW-114A) which consists of a photocathode (S-4 or S-20) and a fine collecting mesh enclosed in a glass vacuum envelope.

The characteristics of a scintillator-photodiode detector are as follows:

(a) Energy response: The active photon absorbing material in this class of detector is a plastic, typically polystyrene or polyvinyl toluene. The generic formula for these plastics is close to $(C_8H_8)_n$. Reference to figure 7 reveals that if this detector is to be used to measure absorbed dose

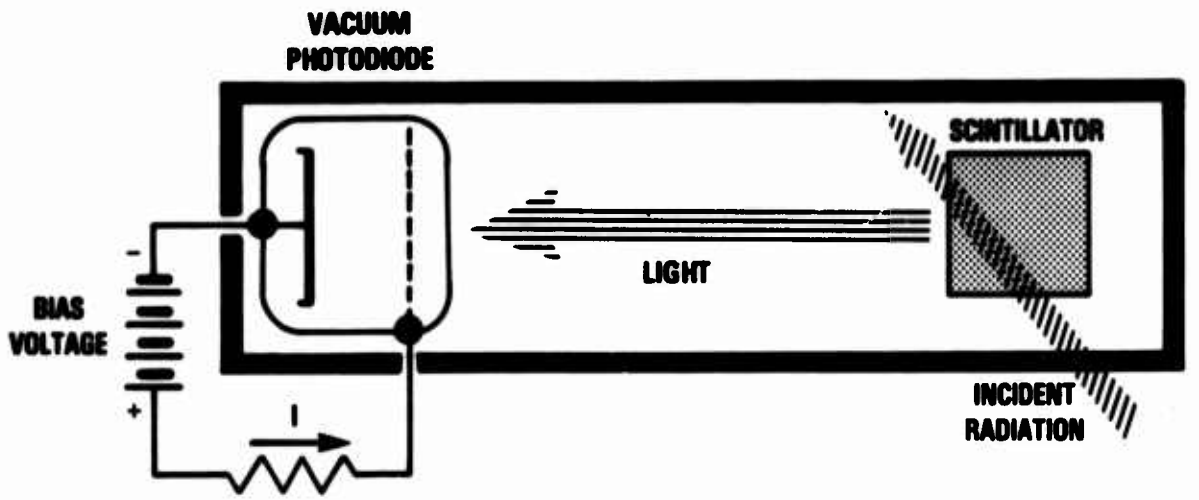

Figure 14. Scintillator-photodiode radiation detector (schematic).

rate in silicon, the photon energy spectrum of the source must not contain any appreciable energy components lower than 200 keV. If there is appreciable photon energy below 200 keV, the detector will underrespond to it and will not faithfully reproduce the true pulse shape.

(b) Time response: The time response of the detector is affected both by the luminescence decay constant of the scintillator and by the time response of the photodetector. The luminescence decay time constant, τ (the light output decays as $\exp[-t/\tau]$), is 1.76 ns for Pilot-B and 2.20 ns for NE-102, two commonly used fast plastic scintillators. The time constant of the FW-114 vacuum photodiode in a low-capacitance holder, 50-Ω system, biased at 5 kV, is 0.28 ns. Thus the time response of the complete detector is essentially the time response of the scintillator.

(c) Linearity: The linearity of the detector is also the combined linearity of the scintillator and the photodetector. The linearity of the light output of the scintillator is affected both by saturation of luminescence centers and by radiation-induced transient darkening of the solvent material, and is thus thickness dependent. The light output of a thin scintillator (0.020 in. of Pilot-B or NE-102) is linear with absorbed dose rate up to about 10^{11} rad(Si)/s. The diode current of the vacuum photodiode is linear to $I_{sat}/2$. I_{sat} depends on the bias voltage. For the FW-114 biased at 5 kV, I_{sat} is 31 A; this detector therefore operates linearly up to a diode current of 15 to 16 A.

(Planar vacuum photodiodes are commercially available from ITT Electro-Optical Products Div., 3700 E. Pontiac St., Ft. Wayne, IN 46803, and from Hamamatsu Corporation, 420 South Ave., Middlesex, NJ 08846. Plastic scintillators are commercially available from Nuclear Enterprises America, 23 Madison Rd., Fairfield, NJ 07006, and from National Diagnostics, 198 Route 206 S., Somerville, NJ 08876.)

4.3 Secondary Emission Detectors

Secondary emission detectors depend for their operation on the collection of photon-induced secondary electrons. The secondary emission monitor (SEM) resembles a thin parallel-plate ionization chamber, except that it is evacuated (see fig. 15a). Secondary electrons (mostly Compton scattered) from the emitter are collected by the collector. The secondary electron current can be related to the photon energy fluence if the photon energy spectrum is known. SEM's are frequently used as transmission pulse-shape monitors at linac facilities, and not as absorbed-dose-rate detectors per se.

The Compton diode resembles the SEM, but it is usually constructed with thick layers of material and may be either evacuated or filled with a dielectric material (see fig. 15b). The emitter and the entrance and exit windows may all be of different materials. The diode current depends on the rather complex balance of the various forward- and back-scattered Compton currents in the diode. Its energy response function may be tailored over a fairly large range by selecting the material types and thicknesses of the various electrodes and the intervening medium. As with the SEM, the Compton

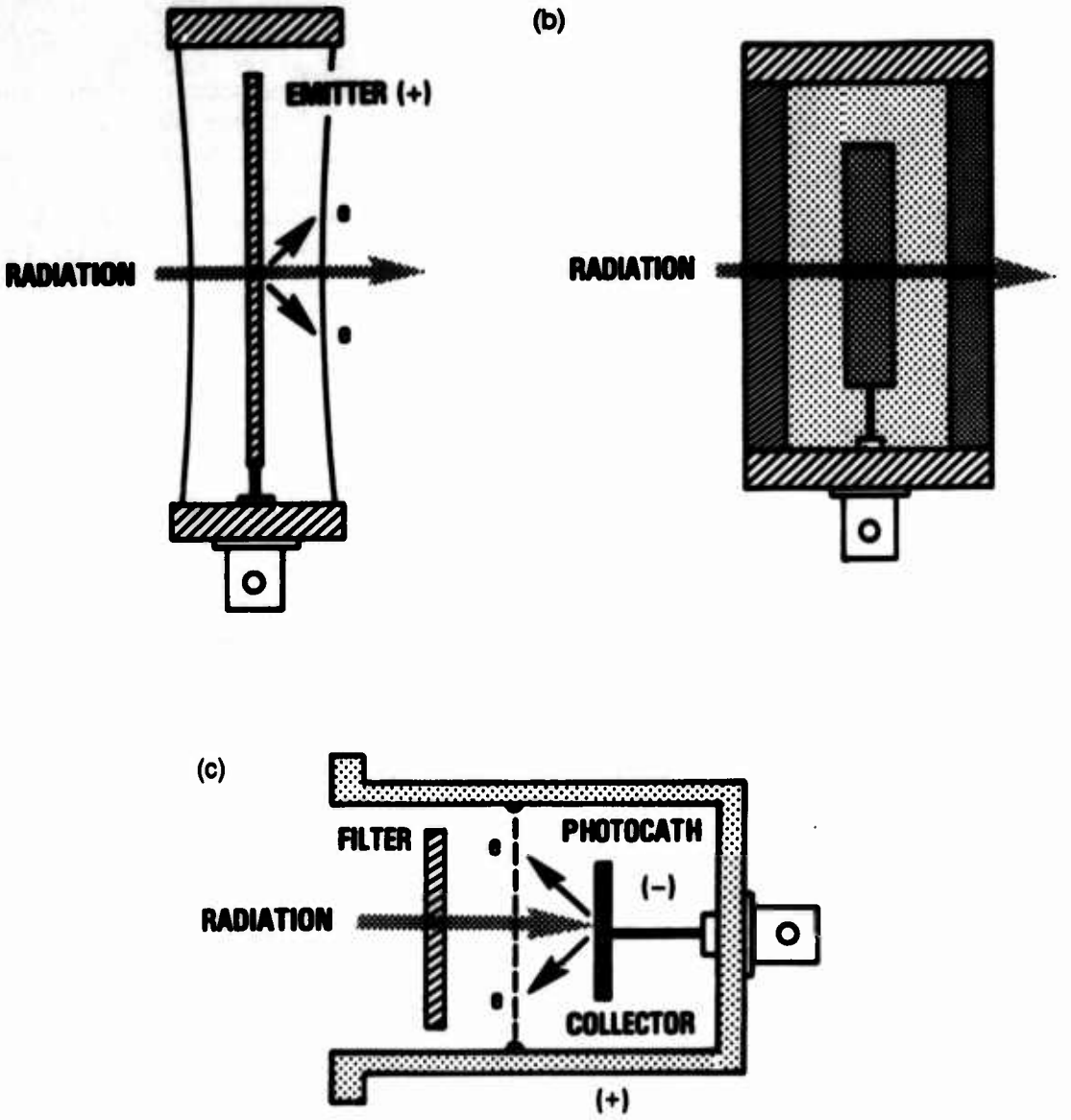

Figure 15. Secondary emission detectors: (a) secondary emission monitor, (b) Compton diode, and (c) x-ray diode (XRD).

diode current can be related to the incident photon energy fluence if the photon spectrum is known. The Compton diode is most useful for measurements in high-energy photon spectra.

The x-ray diode (XRD) consists of a photocathode, a thin collector mesh, and an optional filter in a high vacuum (see fig. 15c). The XRD is most commonly used for very low energy photon spectra ($h\nu$ < 100 keV) because it depends for its operation on the collection of photoelectrons emitted by the photocathode. The energy response function of the XRD is strongly affected by the energy of the K-absorption edges of the photocathode and filter materials.

5. MEASUREMENT OF THE SPECTRUM

There are two approaches to the determination of a photon energy spectrum: measurement and calculation. Unfortunately, both of these approaches are very difficult, costly, and time consuming, and require a high degree of specialized expertise. For these reasons, an accurate determination of a flash x-ray or radioisotope spectrum is generally beyond the means of the radiation hardness tester, and such data exist mostly for large, well-staffed radiation testing facilities. The possible techniques for determining the photon energy spectrum are briefly discussed below.

5.1 Experimetal Methods

Experimental methods which are feasible in the energy region of interest to radiation effects testing employ magnetic Compton spectrometers, absorption spectrometers, and K-edge detectors.

Magnetic Compton spectrometer.--This device is useful for spectra spanning the 200-keV to 10-MeV range. In this device a tightly collimated beam of photons passes through a magnetic field to sweep out any electrons. It then strikes a thin, low-Z scattering foil (e.g., Be). Compton scattered electrons emitted at some predetermined angle are collimated and their energy analyzed using a magnetic electron spectrometer. The photon energy spectrum can be calculated using (1) the known Klein-Nishina cross section for Compton scattering, (2) multiple scattering and the continuous slowing down approximation for the electrons escaping from the foil, and (3) the electron detector response functions.

The disadvantage of this technique is that it is intrinsically very inefficient. A practical Compton spectrometer can be constructed which will detect one energy-analyzed electron for each 10^8 photons/cm^2 incident on the scattering foil. This means that in order to achieve a signal-to-noise ratio of unity, only one out of every 10^8 incident stray electrons may be allowed to reach the electron detectors. This requires very extensive shielding around the spectrometer, making it large, massive, and expensive. A second disadvantage is the extremely tight photon collimation required, essentially limiting this technique to point sources of photons with a relatively long unobstructed line of sight. Nevertheless, this technique has been used to measure the photon energy spectrum of a 10-MV flash x-ray generator on at least one occasion with good results (Kelly et al, 1971).

Absorption spectrometers. The principle underlying this technique is to have an array of identical detectors, each of which has a different thickness and/or type of absorber interposed between it and the photon beam. The spectrum is then "unfolded" from the array of detector responses. The difficulties inherent in this technique are

(a) producing a number of absorber/detector combinations which have sufficiently different energy response functions over the spectral range of interest, and

(b) developing an "unfolding" algorithm which leads to a physically meaningful solution. If we let the unknown spectrum be $\phi(E)$, the energy response function of the i^{th} detector be $R_i(E)$, and the measured detector response of the i^{th} detector when exposed to the unknown spectrum be Q_i, then Q_i is related to $\phi(E)$ by

$$Q_i = \int \phi(E) R_i(E)\, dE \quad . \tag{22}$$

Such a system of integral equations cannot in general be solved for $\phi(E)$, given a set of n Q_i and $R_i(E)$.

All practical unfolding algorithms therefore use the iterative unfolding technique; that is, a trial spectrum is mathematically propagated through the spectrometer and the calculated detector responses are compared with the measured data. The trial spectrum is adjusted and the process is repeated until the result converges to a "solution."

This method has not produced satisfactory results in the past; however, Kerris and Gorbics (1985) recently reported good success with 1- to 2-MV flash x-ray spectra as well as Co^{60} spectra, using carefully calibrated TLD's in spherical absorber shells and an improved iterative unfolding code. This technique appears to be applicable to the energy range from 10 keV to 1 MeV.

K-edge detectors.--A K-edge detector consists of a detector of a certain atomic number, Z_D, which has its peak photon sensitivity at energies just above its K-absorption edge. If a photon beam is passed through a filter of atomic number Z_F, where $Z_F > Z_D$, then the detector will have a fairly narrow energy response, lying roughly between the two K-absorption edges of Z_D and Z_F. An array of such detectors can cover the region from ~1 keV to the K-absorption edge of uranium at 116 keV.

5.2 Calculational Methods

If the energy spectrum of the original source particles (electrons for flash x-ray sources, nuclear gamma rays for Co^{60}) and the characteristics of all intervening materials are known, then the photon energy spectrum at any given point can be calculated by means of a coupled electron-photon Monte Carlo code, such as TIGER (Halbleib and Melhorn, 1984). Although these codes are somewhat complex, and require a lot of computer time for statistically good results, such calculations often give the only reliable or practically achievable data on the energy spectrum for a particular irradiator configuration (Sanford and Halbleib, 1984; Woolf et al, 1983, 1984). The work of Kelley et al (1971) has shown that such transport code calculations give results which are in good agreement with the much more difficult Compton spectrometer measurements.

6. APPLICATION TO ELECTRONIC DEVICE TESTING

In the preceding three sections I have tried to give some detailed guidance for measuring the equilibrium absorbed dose and dose rate in a reference

material, and some procedures for determing the photon energy spectrum of the source. It still remains to translate this information into absorbed dose at the region of interest in the test object.

For high-energy photon sources such as 5- to 10-MV flash x-ray generators or linacs, there is not much difficulty in doing this. Interface dose enhancement can be minimized by proper orientation of the test object, and the dose can be found by application of equation (16).

For low-energy photon sources such as flash x-ray generators of ≤1.5 MV accelerating potential, there is a considerable but unavoidable problem. The dose in the region of interest must be calculated from the known test object parameters, the photon energy spectrum to the extent that it is known, and the equilibrium dose or dose rate measured in some reference material at the location of interest in the radiation field.

An intermediate-energy case of considerable practical interest is that of absorbed dose measurements made in Co^{60} facilities. For some time such measurements were thought to fall into the simple high-photon-energy classification; this supposition would indeed be true if the photon radiation from Co^{60} sources consisted exclusively of 1.17- and 1.33-MeV gamma rays. However it is now generally recognized that the finite thickness of sources, as well as the encapsulation materials and other surrounding structures which are inevitably present in irradiators, can contribute a substantial amount of low-energy gamma radiation, principally by Compton scattering (Woolf et al, 1983, 1984). It is this low-energy photon component which can introduce significant device dosimetry errors because the equilibrium dose as measured by a dosimeter can be quite different from the dose deposited in the device under test, because of dose enhancement (Brown and Dozier, 1982; Long et al, 1982).

If there is an appreciable low-energy spectral component present in a particular irradiator configuration, special experimental techniques can be employed to ensure that dosimetry measurements adequately represent the dose in the test device (Brown and Dozier, 1982); these techniques are also described in a soon-to-be published ASTM standard, entitled Standard Practice for Minimizing Dosimetry Errors in Radiation Hardness Testing of Electronic Devices Using Co-60 Sources. A two-step process is required:

(a) The test object (device) must be enclosed in a filter box with an outer layer of 0.063 in. of lead followed by 0.030 in. of aluminum. This filter will remove most of the low-energy photons, minimizing low-energy dose enhancement.

(b) The test device must be oriented so that the plane of the semiconductor chip is perpendicular to the direction of the radiation, and with the higher atomic number layers (if any) toward the source of radiation. This will minimize dose enhancement error due to high-energy photons.

An experimental technique has been developed which permits us to determine whether any given Co^{60} source geometry has an appreciable low-energy photon component. A special ionization chamber which has interchangeable aluminum

and gold-aluminum electrodes is required to make these measurements. Two ionization current measurements are made in the Co^{60} environment to be tested, one with gold-aluminum electrodes, one with plain aluminum electrodes. The ratio I_{Au}/I_{Al} is strongly indicative of the spectral purity of the Co^{60} source configuration under test, and can easily be related to an upper limit of dose enhancement which may be expected. The technique for doing this is described by Kerris and Gorbics (1985), and also in a soon-to-be published ASTM standard, entitled Standard Practice for the Application of Ionization Chambers for Assessing the Importance of the Low Energy Gamma Component of Cobalt-60 Irradiators Used in Radiation-Hardness Testing of Electronic Devices.

REFERENCES

ASTM Standard E665: Standard Practice for Determining Absorbed Dose versus Depth in Materials Exposed to the X-ray Output of Flash X-ray Machines, 1985 Annual Book of ASTM Standards, vol. 12.02, American Society for Testing and Materials (ASTM), Philadelphia (1985), p 348.

ASTM Standard E666: Standard Practice for Calculating Absorbed Dose from Gamma or X Radiation, 1985 Annual Book of ASTM Standards, vol. 12.02, ASTM, Philadelphia (1985), p 352.

ASTM Standard E668: Standard Practice for the Application of Thermoluminescence Dosimetry (TLD) Systems for Determining Absorbed Dose in Radiation-Hardness Testing of Electronic Devices, 1985 Annual Book of ASTM Standards, vol. 12.02, ASTM, Philadelphia (1985), p 360.

ASTM Standard E170: Standard Terminology Relating to Radiation Measurements and Dosimetry, 1985 Annual Book of ASTM Standards, vol. 12.02, ASTM, Philadelphia (1985), p 25.

Attix, F. H., Thermoluminescence Dosimetry with Calcium Fluoride, in Manual on Radiation Dosimetry, N. W. Holm and R. J. Berry, ed., Marcel Dekker, Inc., New York (1970).

Becker, K., Solid State Dosimetry, ch. 2, Thermoluminescence, CRC Press, Cleveland (1973).

Brown, D. B., and C. M. Dozier, Reducing Errors in Dosimetry Caused by Low-Energy Components of Co-60 and Flash X-ray Sources, IEEE Trans. Nucl. Sci., NS-29 (1982), 1996.

Burke, E. A., and J. C. Garth, An Algorithm for Energy Deposition at Interfaces, IEEE Trans. Nucl. Sci., NS-23 (1976), 1838.

Burlin, T. E., Cavity Chamber Theory, ch. 8 in Radiation Dosimetry, 2nd ed., vol. 1, F. H. Attix and W. C. Roesch, ed., Academic Press, New York (1969).

Burlin, T. E., The Theory of Dosimeter Response with Particular Reference to Ionization Chambers, ch. 2 in Manual on Radiation Dosimetry, N. W. Holm and R. J. Berry, ed., Marcel Dekker, Inc., New York (1970).

Cameron, J. R., Lithium Fluoride Thermoluminescent Dosimetry, in Manual on Radiation Dosimetry, N. W. Holm and R. J. Berry, ed., Marcel Dekker, Inc., New York (1970).

Chadsey, W. L., X-ray Dose Enhancement, IEEE Trans. Nucl. Sci., NS-25 (1978), 1591.

Fowler, J. F., and F. H. Attix, Solid State Integrating Dosimeters, ch. 13 in Radiation Dosimetry, 2nd ed., vol. 2, Instrumentation, F. H. Attix and W. C. Roesch, ed., Academic Press, New York (1966).

Garth, J. C., W. L. Chadsey, and R. L. Sheppard, Monte Carlo Analysis of Dose Profiles Near Photon Irradiated Material Interfaces, IEEE Trans. Nucl. Sci., NS-22 (1975), 2562.

Gorbics, S. G., F. H. Attix, and K. G. Kerris, Thermoluminescent Dosimeters for High-Dose Applications, Health Physics, 25 (1973), 499.

Halbleib, J. A., and T. A. Melhorn, ITS: The Integrated TIGER Series of Coupled Electron/Photon Monte Carlo Transport Codes, Sandia Report SAND84-0573, Sandia National Laboratories, Albuquerque (1984).

Hubbell, J. H., Photon Cross Sections, Attenuation Coefficients, and Energy Absorption Coefficients from 10 keV to 100 GeV, NSRDS-NBS Handbook 29, National Bureau of Standards, Washington (1969).

ICRU Report 33, Radiation Quantities and Units, International Commission on Radiation Units and Measurements, Washington (1980).

Kelley, J. G., L. D. Posey, and J. A. Halbleib, A Magnetic Compton Spectrometer for High-Intensity Pulsed Gamma Environments, IEEE Trans. Nucl. Sci., NS-18, No. 2 (February 1971), 131.

Kerris, K. G., and S. G. Gorbics, Experimental Determination of the Low-Energy Spectral Component of Cobalt-60 Sources, IEEE Trans. Nucl. Sci., NS-32 (1985), 4356.

Long, D. M., D. G. Millward, and J. Wallace, Dose Enhancement Effects in Semiconductor Devices, IEEE Trans. Nucl. Sci., NS-29 (1982), 1980.

McLaughlin, W. L., and L. Chalkley, Measurement of Radiation Dose Distributions with Photochromic Materials, Radiology, 84 (1965), 124.

McLaughlin, W. L., Radiochromic Dye-Cyanide Dosimeters, in Manual on Radiation Dosimetry, N. W. Holm and R. J. Berry, ed., Marcel Dekker, Inc., New York (1970).

McLaughlin, W. L., Dosimetry, ch. 8 in Preservation of Food by Ionizing Radiation, vol. 1, E. S. Josephson and M. S. Peterson, ed., CRC Press, Boca Raton (1982).

Roesch, W. C., and F. H. Attix, Basic Concepts of Dosimetry, ch. 1 in Radiation Dosimetry, 2nd ed., vol. 1, Fundamentals, F. H. Attix and W. C. Roesch, ed., Academic Press, New York (1968).

Sanford, T. W. L., and J. A. Halbleib, Radiation Output and Dose Predictions for Flash X-ray Sources, IEEE Trans. Nucl. Sci., NS-31 (1984), 1095.

Wall, J. A., and E. A. Burke, Gamma Dose Distribution at and Near the Interface of Different Materials, IEEE Trans. Nucl. Sci., NS-17 (December 1970), 305.

Whittaker, B., Red Perspex Dosimetry, in Manual on Radiation Dosimetry, N. W. Holm and R. J. Berry, ed., Marcel Dekker, Inc., New York (1970).

Woolf, S., and A. R. Frederickson, Photon Spectra in Co-60 Gamma Test Cells, IEEE Trans. Nucl. Sci., NS-30 (1983), 4371.

Woolf, S., and E. A. Burke, Monte Carlo Calculations of Irradiation Test Photon Spectra, IEEE Trans. Nucl. Sci., NS-31 (1984), 1089.

DISTRIBUTION

ADMINISTRATOR
DEFENSE TECHNICAL INFORMATION CENTER
ATTN DTIC-DDA (12 COPIES)
CAMERON STATION, BUILDING 5
ALEXANDRIA, VA 22304-6145

COMMANDER
US ARMY COMBAT SYSTEMS
TEST ACTIVITY
ATTN C. HEIMBACH
BLDG 860 STECS-NE
ABERDEEN PROVING GROUND, MD 21005-5059

NVEOL
ATTN DELNV-IRT, A. J. KENNEDY
FT BELVOIR, VA 22060

WHITE SANDS MISSILE RANGE
PO BOX 215
ATTN DR. J. MEASON
WHITE SANDS MISSILE RANGE, NM 88002

WHITE SANDS MISSILE RANGE
PO BOX 333
ATTN DR. W. W. SALLEE
WHITE SANDS, NM 88002

NAVAL RESEARCH LABORATORY
REACTOR MATERIALS BRANCH
ATTN CODE 6290, L. E. STEELE, HEAD
WASHINGTON, DC 20375

NAVAL RESEARCH LABORATORY
ATTN CODE 6680, DR. DENNIS BROWN
ATTN CODE 6464, F. J. CAMPBELL
ATTN CODE 6682, DR. C. M. DOZIER
ATTN CODE 6070, S. G. GORBICS, (20 COPIES)
WASHINGTON, DC 20375

RADC/ESR
ATTN J. C. GARTH
HANSCOM AFB, MA 01731

NASA GODDARD SPACE FLIGHT CENTER
ATTN CODE 754, V. DANCHENKO
ATTN CODE 754, S. BRASHEARS
GREENBELT, MD 20771

NASA LANGLEY RESEARCH CENTER
ATTN SHIELA ANN L. LONG
MS 399
HAMPTON, VA 23665

BATTELLE PACIFIC NORTHWEST LABORATORY
PO BOX 999
ATTN DR. P. L. ROBERSON
SENIOR RESEARCH SCIENTIST
RADIOLOGICAL SCIENCE DEPARTMENT
318 BUILDING, 300 AREA
RICHLAND, WA 99352

BALLISTIC RESEARCH LABS
ATTN A. H. KAZI
ABERDEEN, MD 21001

HANFORD ENGINEERING DEVELOPMENT LAB
PO BOX 1970
ATTN DR. W. N. McELROY
CHAIRMAN, ASTM E10.05
300 AREA
RICHLAND, WA 99352

JPL
M/S T-1180
ATTN M. GAUTHIER
4800 OAK GROVE DRIVE
PASADENA, CA 91109

JET PROPULSION LABORATORY
ATTN J. W. WINSLOW
MS 144-218
4800 OAK GROVE DRIVE
PASADENA, CA 91103

JET PROPULSION LABORATORY
CALIFORNIA INSTITUTE OF TECHNOLOGY
ATTN W. E. PRICE
4800 OAK GROVE DRIVE
PASADENA, CA 91109

MAXWELL LABS, INC
ATTN J. E. RAUCH
9244 BALBOA AVE
SAN DIEGO, CA 92123

PACIFIC NORTHWEST LAB
PO BOX 999
ATTN W. C. MORGAN
RICHLAND, WA 99352

PNL
PO BOX 999
ATTN DR. J. L. BRIMHALL
RICHLAND, WA 99352

RISO NATIONAL LABORATORY
ACCELERATOR DEPARTMENT
PO BOX 49
ATTN DR. A. MILLER
DK-4000 ROSKILDE, DENMARK

SANDIA LABS.
PO BOX 5800
ATTN W. H. BUCKELEW, ORG. 6446
ATTN DR. J. A. HALBLEIB, SR, DIV 4231
ATTN J. G. KELLY, DIV. 1232
ATTN DR. T. F. LUERA, DIV 6451
ATTN L. D. POSEY, DIV 1232
ALBUQUERQUE, NM 87185

DISTRIBUTION (cont'd)

SANDIA NATIONAL LABORATORIES
RADIATION DOSIMETRY LABORATORY
EXPERIMENTAL SYSTEMS DESIGN
DIVISION 6452
ATTN DR. D. W. VEHAR
ALBUQUERQUE, NM 87185

AECL RADIOCHEMICAL COMPANY
SENIOR RADIATION PHYSICIST
PO BOX 13500
ATTN R. CHU
KANATA, ONT, CANADA K2K 1X8

AEROJET NUCLEAR CE
ATTN J. M. BEESTON
1604 CHARLENE STREET
IDAHO FALLS, ID 83401

ARACOR
ATTN L. J. PALKUTI
1223 E. ARQUES AVE
SUNNYVALE, CA 94086

ARCON CORPORATION
ATTN S. WOOLF
260 BEAR HILL ROAD
WALTHAM, MA 02154

ATOMIC ENERGY OF CANADA, LTD.
PO BOX 6300, STATION J
ATTN B. J. JACKSON
OTTAWA, CANADA K2A 3W3

ATOMIC ENERGY OF CANADA, LTD.
ATTN DR. K. MEHTA
PINAWA, MANITOBA
CANADA ROE 1LO

BABCOCK & WILCOX CO
PO BOX 1260
ATTN R. H. LEWIS
LYNCHBURG, VA 24505

BATTELLE PROJECT MANAGEMENT DIV
ATTN DR. J. PERRIN
505 KING AVENUE
COLUMBUS, OH 43201

BOEING COMPANY
ATTN ROGER C. KENNEDY
MS 2R-GV, PO BOX 3999
SEATTLE, WA 98124

BOEING AEROSPACE CO
ORGN 2-5310, MS 2R-00
ATTN R. GUAY
SEATTLE, WA 98124

BOEING CO
ATTN RONALD FUSCH
MS 2R-GV, PO BOX 3999
SEATTLE, WA 98124

BOEING AEROSPACE CO
PO BOX 3999
ATTN ITSU ARIMURA
SEATTLE, WA 98124

GENERAL MANAGER
RADIATION-STERILIZERS, INC
ATTN DR. B. P. FAIRAND
305 ENTERPRISE DRIVE
WESTERVILLE, OH 43081

IRT CORPORATION
LINAC FACILITY
ATTN D. E. WILLIS, MANAGER
7695 FORMULA PLACE
SAN DIEGO, CA 92121

IRT CORP
PO BOX 80817
ATTN J. HARRITY
SAN DIEGO, CA 92138

JAYCOR
PO BOX 85154
ATTN DR. B. C. PASSENHEIM
11011 TORREYANA ROAD
SAN DIEGO, CA 92138

JOHNSON & JOHNSON RESEARCH
ATTN T. A. OLEJNIK
21 LAKE DRIVEE. WINDSOR, NJ 08520

KAMAN-TEMPO
ATTN DR. E. WOLICKI
2560 HUNTINGTON AVENUE
SUITE 500
ALEXANDRIA, VA 22303

KAMAN TEMPO
ATTN W. A. ALFONTE
2560 HUNTINGTON AVE
SUITE 506
ALEXANDRIA, VA 22303

G. MESSENGER
3111 BEL AIR DRIVE
LAS VEGAS, NV 89109

MISSION RESEARCH CORP
ATTN E. A. BURKE
74 NORTHEASTERN BLVD
NASHUA, NH 03062

DISTRIBUTION (cont'd)

MISSION RESEARCH CORPORATION
ATTN DR. E. A. BURKE
11 INDIAN HILL ROAD
WOBURN, MA 01801

NORTHROP CORPORATION
ONE RESEARCH PARK
ATTN DR. J. R. SROUR
PALOS VERDES PENINSULA, CA 90274

NORTHROP CORPORATION
ELECTRONICS DIVISION
ATTN B. T. AHLPORT
2301 W. 120TH STREET
HAWTHORNE, CA 90250

RADIATION DYNAMICS INC.
ENGINEERING DEPARTMENT
ATTN M. STRELCZYK
EXPERIMENTAL APPLICATIONS PHYSICIST
316 SOUTH SERVICE RD
MELVILLE, NY 11747

RAYTHEON CO
EQUIPMENT DEVELOPMENT LABORATORIES
ATTN R. N. DIETTE
ATTN B. W. SCHUPP
528 BOSTON POST ROAD
SUDBURY, MA 01776

ROCKWELL
PO BOX 1449
ATTN P. S. OLSON
CANOGA PARK, CA 91304

ROCKWELL INTERNATIONAL
MANAGER, APPLIED NUCLEAR RESEARCH
ROCKETDYNE DIVISION, NA02
ATTN DR. H. FARRAR IV
6633 CANOGA AVENUE
CANOGA PARK, CA 91304

SCIENCE APPLICATIONS, INC
ATTN DR. V. V. VERBINSKI
1200 PROSPECT STREET
LA JOLLA, CA 93027

TRW DEFENSE SYSTEMS GROUP
ONE SPACE PARK
ATTN R. D. LOVELAND
REDONDO BEACH, CA 90278

UNION CARBIDE COMPANY
NUCLEAR DIVISION
PO BOX X
ATTN F. B. K. KAM
OAK RIDGE, TN 37830

WESTINGHOUSE HANFORD CO
ATTN H. R. BRAGER
326 BLD. W/A-57, BOX 1970
RICHLAND, WA 99352

WESTINGHOUSE HANFORD CO
ATTN DR. F. A. GARNER
326 BLDG 300, AREA W/a-57
RICHLAND, WA 99352

WESTINGHOUSE HANFORD CO
BOX 1970
ATTN F. R. SHOBER
RICHLAND, WA 99352

UNIVERSITY OF ARKANSAS
MECHANICAL ENGINEERING DEPARTMENT
ATTN DR. J. G. WILLIAMS
FAYETTEVILLE, AR 72701

UNIVERSITY OF MARYLAND
INSTITUTE FOR PHYSICAL SCIENCE
TECHNOLOGY
ATTN DR. W. J. CHAPPAS
COLLEGE PARK, MD 20742

NATIONAL BUREAU OF STANDARDS
ATTN DR. R. S. CASWELL, 245/B109
ATTN DR. S. E. CHAPPELL, ADMIN/A625
ATTN W. L. McLAUGHLIN, 245/C216
ATTN DR. J. W. MOTZ, 245/C216
ATTN J. C. HUMPHREYS, 245/C216
GAITHERSBURG, MD 20899

US ARMY LABORATORY COMMAND
ATTN TECHNICAL DIRECTOR, AMSLC-TD

INSTALLATION SUPPORT ACTIVITY
ATTN RECORD COPY, SLCIS-IM-TS
ATTN LIBRARY, SLCIS-IM-TL (3 COPIES)
ATTN LIBRARY, SLCIS-IM-TL (WOODBRIDGE)
ATTN TECHNICAL REPORTS BRANCH, SLCIS-IM-TR
ATTN LEGAL OFFICE, SLCIS-CC

HARRY DIAMOND LABORATORIES
ATTN D/DIVISION DIRECTORS
ATTN CHIEF, SLCHD-NW-E
ATTN CHIEF, SLCHD-NW-EC
ATTN CHIEF, SLCHD-NW-EE
ATTN CHIEF, SLCHD-NW-R
ATTN CHIEF, SLCHD-NW-RA
ATTN CHIEF, SLCHD-NW-RC
ATTN CHIEF, SLCHD-NW-RE
ATTN CHIEF, SLCHD-NW-RH
ATTN CHIEF, SLCHD-NW-RI
ATTN CHIEF, SLCHD-NW-P

DISTRIBUTION (cont'd)

HARRY DIAMOND LABORATORIES (cont'd)
ATTN B. ZABLUDOWSKI, SLCHD-IT-E
ATTN J. R. ROSADO, SLCHD-NW
ATTN R. J. REYZER, SLCHD-NW-EC
ATTN L. ROUNDS, SLCHD-NW-P
ATTN J. CORRIGAN, SLCHD-NW-P
ATTN S. SHARE, SLCHD-NW-RA
ATTN W. VAULT, SLCHD-NW-RA
ATTN J. BENEDETTO, SLCHD-NW-RC
ATTN H. BOESCH, SLCHD-NW-RC
ATTN A. J. LELIS, SLCHD-NW-RC
ATTN J. McGARRITY, SLCHD-NW-RC
ATTN F. McLEAN, SLCHD-NW-RC
ATTN T. OLDHAM, SLCHD-NW-RC
ATTN M. BUMBAUGH, SLCHD-NW-RH
ATTN H. EISEN, SLCHD-NW-RH
ATTN J. HALPIN, SLCHD-NW-RH
ATTN R. GILBERT, SLCHD-NW-RH
ATTN J. BLACKBURN, SLCHD-NW-RH
ATTN G. MERKEL, SLCHD-NW-RH
ATTN S. RATTNER, SLCHD-NW-RH
ATTN C. SELF, SLCHD-NW-RH
ATTN F. J. AGEE, SLCHD-NW-RI
ATTN C. CASAER, SLCHD-NW-RI
ATTN D. DAVIS, SLCHD-NW-RI
ATTN S. GRAYBILL, SLCHD-NW-RI
ATTN G. HUTTLIN, SLCHD-NW-RI
ATTN P. SARIGIANIS, SLCHD-NW-RI
ATTN D. WHITTAKER, SLCHD-NW-RI
ATTN K. KERRIS, SLCHD-NW-RI (100 COPIES)